

Limits on radio emission from pulsar wind nebulae

B. M. Gaensler,^{1*} B. W. Stappers,² D. A. Frail,³ D. A. Moffett,^{4†}
S. Johnston⁵ and S. Chatterjee^{6,3}

¹Center for Space Research, Massachusetts Institute of Technology, 70 Vassar Street, Cambridge, MA 02139, USA; bmg@space.mit.edu

²Astronomical Institute “Anton Pannekoek”, Kruislaan 403, 1098 SJ Amsterdam, The Netherlands

³National Radio Astronomy Observatory, P.O. Box 0, Socorro, NM 87801, USA

⁴Physics Department, University of Tasmania, GPO Box 252-21, Hobart, Tasmania 7001, Australia

⁵Research Centre for Theoretical Astrophysics, University of Sydney, NSW 2006, Australia

⁶Department of Astronomy and Space Sciences, Cornell University, Ithaca, NY 14853, USA

25 October 2018

ABSTRACT

We report on a sensitive survey for radio pulsar wind nebulae (PWN) towards 27 energetic and/or high velocity pulsars. Observations were carried out at 1.4 GHz using the Very Large Array and the Australia Telescope Compact Array, and utilised pulsar-gating to search for off-pulse emission. These observing parameters resulted in a considerably more sensitive search than previous surveys, and could detect PWN over a much wider range of spatial scales (and hence ambient densities and pulsar velocities). However, no emission clearly corresponding to a PWN was discovered. Based on these non-detections we argue that the young and energetic pulsars in our sample have winds typical of young pulsars, but produce unobservable PWN because they reside in low density ($n \sim 0.003 \text{ cm}^{-3}$) regions of the ISM. However, non-detections of PWN around older and less energetic pulsars can only be explained if the radio luminosity of their winds is less than 10^{-5} of their spin-down luminosity, implying an efficiency at least an order of magnitude smaller than that seen for young pulsars.

Key words: ISM: general – pulsars: general – radio continuum: ISM – stars: winds – supernova remnants

1 INTRODUCTION

Almost all radio pulsars have rotational periods which are steadily increasing with time. This spin down corresponds to a loss of rotational kinetic energy $\dot{E} \equiv 4\pi^2 I \dot{P}/P^3$, where I is the moment of inertia of the neutron star (assumed to be 10^{45} g cm^2) and P is its period; for the known pulsar population \dot{E} falls in the range $10^{28} - 10^{39} \text{ erg s}^{-1}$. The bolometric luminosity of the radio pulses themselves is in all cases a tiny fraction of the spin-down luminosity \dot{E} , and it is thought that most of the pulsar’s spin-down luminosity is dissipated via a magnetised wind populated by relativistic electrons and positrons (Rees & Gunn 1974; Michel 1982; Kennel & Coroniti 1984). However it is still not well understood how this wind is produced, how it evolves as it flows away from the pulsar, what it is composed of, how its prop-

erties depend on those of the pulsar itself, or how it changes as the pulsar ages.

Particles in the wind move along magnetic field lines as they stream away from the pulsar magnetosphere, and produce no observable emission. At some distance from the pulsar, the pressure of the wind is eventually balanced by an external pressure, and the resulting shock randomises the pitch angles of the relativistic particles. These particles consequently gyrate in the local magnetic field and produce synchrotron emission. The properties of the resulting *pulsar wind nebula* (PWN) can then be used to determine various parameters of the pulsar wind which produces it. At radio wavelengths, PWN are characterised by an amorphous or filled-centre morphology, a moderate degree of linear polarization ($\sim 20\%$), and relatively flat spectra ($\alpha \sim -0.3$, $S_\nu \propto \nu^\alpha$) (Weiler & Panagia 1978).

Various types of PWN are produced, depending on the source of confinement of the wind. Young pulsars are often still located inside their associated supernova remnants (SNRs), and the hot gas produced by the SNR blast-wave provides the confining pressure. These PWN, also known as

* Hubble Fellow

† Current address: Physics Department, Furman University, 3300 Pointsett Hwy, Greenville, SC 29613, USA

“plerions”, are typified by the Crab Nebula. If the SNR has dissipated, the confining pressure is then that of the ambient interstellar medium (ISM). This results in much larger “ghost remnants”, which have been proposed but not observed (Blandford et al. 1973; Cohen et al. 1983). In cases where a pulsar has a high space velocity, the ram pressure resulting from its motion can dominate the ambient gas pressure, resulting in a bow-shock PWN (e.g. Frail & Kulkarni 1991).

While PWN can tell us much about pulsar winds, the number of sources we have to study is small – at radio wavelengths, fewer than 10 pulsars have observable PWN. All of these pulsars are very young and have high values of \dot{E} . While $\sim 20\%$ of SNRs have a “plerionic” component, in most cases the associated pulsar has not been detected, and without knowing the pulsar parameters it is difficult to constrain the properties of the PWN and the corresponding wind. Thus it is of considerable interest to target candidate pulsars with the intention of either finding new PWN, or determining upper limits on such emission.

Many searches for radio PWN around energetic or fast-moving pulsars have been carried out, at varying resolutions and surface-brightness sensitivities, but usually with no success (e.g. Schönhardt 1974; Weiler, Goss & Schwarz 1974; Cohen et al. 1983). The most recent and comprehensive of these searches, and the only one to specifically target young, energetic or high velocity pulsars, was the recent survey of Frail & Scharringhausen (1997), hereafter FS97. FS97 imaged regions around 35 pulsars with the Very Large Array (VLA) at 8.4 GHz, and found no nebular emission associated with any of their targets. Their stringent upper limits allowed them to conclude that most pulsars put less than 10^{-6} of \dot{E} into radio emission from a PWN, ~ 100 times less than observed for the young, high \dot{E} , pulsars which power detected radio nebulae. Based on this result, FS97 concluded that pulsar winds change in some way as pulsars age and slow down, such that they are no longer efficient at producing radio emission.

However, despite these apparently constraining limits, in hindsight the observing parameters for this search were probably not ideal for looking for PWN. First, FS97 argued that for ambient densities of 1 cm^{-3} and pulsar velocities of 150 km s^{-1} , PWN around almost all their sources were likely to be unresolved, even at their high spatial resolution of $0''.8$. However, other choices of ambient density and pulsar velocity can produce PWN with much larger angular extents, resulting in a flux density limit much poorer than estimated by FS97. Furthermore, the maximum scale to which FS97 were sensitive was only $20''$; they could not detect PWN larger than this at any flux density. Secondly, in 40% of their sample FS97 detected a point source at the position of the pulsar, but had no way of distinguishing between the compact PWN they were looking for and the pulsars themselves. By extrapolating pulsar flux densities from much lower frequencies, FS97 argued that the flux densities they were detecting at 8.4 GHz were consistent with the expected pulsed fluxes, and hence concluded that they were not detecting any PWN in these data. Finally, a typical PWN (spectral index $\alpha = -0.3$) has a significantly lower flux density at their observing frequency of 8.4 GHz than at lower frequencies.

Motivated by these points, we have undertaken an ex-

tensive survey for PWN at both northern and southern declinations, with observing parameters chosen to give much greater sensitivity to PWN. First, we have observed at 1.4 GHz, at which frequency PWN can be expected to be $\sim 70\%$ brighter than at 8.4 GHz. Secondly, we have observed at a reduced spatial resolution of $\sim 12''$, to give better sensitivity to extended structure. Thirdly, our observations are in telescope configurations whose shortest spacings correspond to a spatial scale of many arcmin. Finally, and most importantly, all our observations have employed pulsar-gating, in which images are made from data taken only when the pulsar is off; we are thus sensitive to compact and unresolved PWN, which might otherwise be masked by the pulsars themselves.

Initial results from this survey, using the Australia Telescope Compact Array (ATCA), have been presented in two previous papers. Gaensler et al. (1998), hereafter GSFJ98, reported the discovery of a faint PWN associated with PSR B0906–49, while Stappers, Gaensler & Johnston (1999), hereafter SGJ99, presented non-detections of PWN towards four pulsars. We here report on the remainder of this survey, consisting of 1.4 GHz pulsar-gated observations of 27 more pulsars, using the VLA and ATCA. In §2, we describe our observations and analysis, while in §3 we present non-detections of PWN towards these sources. In §4 we quantify the improvement in sensitivity of the current survey, and discuss the constraints we can put on the radio luminosities of pulsar winds from our data.

2 OBSERVATIONS AND REDUCTION

The 27 pulsars observed are listed in Table 1; all were chosen for their high \dot{E} and/or space velocity. From this sample 22 pulsars were observed with the VLA (Napier, Thompson & Ekers 1983), while the remaining 5 pulsars were observed with the ATCA (Frater, Brooks & Whiteoak 1992). All observations were carried out at frequencies near 1.4 GHz.

The VLA observations were made in the C configuration, using a bandwidth of 25 MHz for $00^{\text{h}} < \text{RA} < 12^{\text{h}}$ and 12.5 MHz otherwise, and with a phase centre corresponding to the catalogued pulsar position. The observing time for each pulsar was typically 15 min. Amplitudes were calibrated using observations of 3C 286 and 3C 48, assuming 1.4 GHz flux densities of 14.9 Jy and 16.3 Jy respectively (where $1 \text{ Jy} = 10^{-26} \text{ W m}^{-2} \text{ Hz}^{-1}$). ATCA observations were made in the 6C configuration, using a bandwidth of 128 MHz (further subdivided into 32 spectral channels); amplitude calibration was carried out using PKS B1934–638 and assuming a 1.4 GHz flux density of 14.9 Jy. For ATCA observations, the phase centre was offset from the pulsar’s catalogued position by $\sim 1'$; each pulsar was observed for approximately 12 hr. Antenna gains and instrumental polarization were calibrated using observations of strong unresolved sources in the vicinity of each pulsar; all four Stokes parameters were recorded.

All observations were gated at the pulsar period in order to look for off-pulse emission at the pulsar position, using ephemerides supplied by A.G. Lyne. For the VLA, gating was carried out by phasing up the array on a nearby calibrator, then integrating on the pulsar for a few minutes. The analogue sum of the signals from all antennas was formed from these data, and then folded at the apparent pulse pe-

Table 1. Pulsars surveyed for PWN. Uncertainties in the last digit are indicated (or are omitted when the uncertainty is less than one in the last digit); positional uncertainties do not include systematic errors due to calibration. Three pulsars were not detected, for reasons discussed in the text. PSR B1706–44 was included as a test case.

Pulsar	Date	Telescope	Pulsar Position (J2000)		Pulsar Flux Density at 1.4 GHz (mJy)	Off-pulse RMS (mJy beam ⁻¹)	θ_{\min} ('')	θ_{\max} (')
			RA	Dec				
B0114+58	1999 Jan 05	VLA	0.47	19 × 10	15
B0136+57	1999 Jan 05	VLA	01:39:19.76(1)	+58:14:31.68(7)	4.8(4)	0.30	18 × 10	15
B0355+54	1999 Jan 05	VLA	03:58:53.680(5)	+54:13:13.63(5)	11(2)	0.26	15 × 10	15
J0538+2817	1999 Jan 05	VLA	05:38:25.090	+28:17:09.41(1)	4.1(2)	0.40	12 × 11	15
B0540+23	1999 Jan 05	VLA	05:43:09.665	+23:29:06.167(1)	32.1(1)	0.42	12 × 11	15
B0611+22	1999 Jan 05	VLA	06:14:17.020	+22:29:56.680(5)	6.9(4)	0.40	12 × 11	15
J0631+1036	1999 Jan 05	VLA	1.8	13 × 12	15
B0656+14	1999 Jan 05	VLA	06:59:48.13(2)	+14:14:21.0(4)	1.5(2)	0.26	12 × 12	15
B0736–40	1999 Feb 21	ATCA	07:38:32.342	–40:42:40.16	87(5)	0.19	17 × 8	4.5
B0740–28	1999 Jan 05	VLA	07:42:49.038	–28:22:43.331(2)	25.7(2)	0.53	30 × 10	15
B1356–60	1999 Mar 10	ATCA	13:59:58.5(6)	–60:38:07.73(9)	12.5(3)	0.29	16 × 10	4.5
B1449–64	1999 Feb 19	ATCA	14:53:32.712(1)	–64:13:15.51(1)	19.5(5)	0.07	11 × 9	4.5
B1508–57	1999 Feb 18	ATCA	15:12:43.041(3)	–57:59:59.94(3)	7.3(7)	0.21	10 × 9	1.8
B1634–45	1999 Feb 21	ATCA	16:37:58.729(9)	–45:53:26.7(2)	1.4(3)	0.16	15 × 9	4.5
B1706–16	1999 Feb 02	VLA	17:09:26.44(1)	–16:40:57.4(3)	6.6(3)	0.50	20 × 12	15
B1706–44	1999 Feb 02	VLA	17:09:42.52(2)	–44:29:06(1)	7.3(7)	0.36	91 × 10	15
B1718–35	1999 Feb 02	VLA	17:21:32.71(3)	–35:32:46.4(7)	5(5)	1.6	51 × 11	15
B1719–37	1999 Feb 02	VLA	17:22:59.04(7)	–37:11:57(2)	1.2(2)	0.53	51 × 11	15
B1727–33	1999 Feb 02	VLA	1.6	40 × 9	15
B1730–37	1999 Feb 02	VLA	17:33:26.74(3)	–37:16:56(1)	2(1)	1.2	45 × 12	15
B1754–24	1999 Feb 02	VLA	17:57:29.371(1)	–24:22:02.22(2)	2.8(1)	0.15	25 × 10	15
B1821–19	1999 Feb 02	VLA	18:24:00.460	–19:45:53.571(2)	8.1(3)	0.19	21 × 11	15
B1823–13	1999 Feb 02	VLA	18:26:13.16(3)	–13:34:49.9(7)	2.2(2)	0.32	16 × 12	15
J1835–1106	1999 Feb 02	VLA	18:35:18.32(2)	–11:06:16.6(4)	3(2)	0.58	16 × 12	15
B1930+22	1999 Feb 02	VLA	19:32:22.63(1)	+22:20:53.3(2)	1.6(2)	0.54	12 × 11	15
B1933+16	1999 Feb 02	VLA	19:35:47.830	+16:16:39.806(1)	75(1)	0.34	13 × 11	15
B2011+38	1999 Feb 02	VLA	20:13:10.341(1)	+38:45:43.225(7)	11(1)	0.82	12 × 10	15
B2148+63	1999 Feb 02	VLA	21:49:58.71(3)	+63:29:44.9(2)	2.9(2)	0.59	14 × 10	15

riod to give an un-dedispersed pulse profile. A gate was then set on-line, such that one IF recorded on-pulse data while the other recorded off-pulse data, effectively giving two bins of possibly uneven size. The smearing due to dispersion across the band was sufficiently small for all pulsars that it was always possible to completely separate on- and off-pulse emission when choosing the gate. For the ATCA, visibilities were recorded at high time-resolution (typically 32 bins per period), and then folded at the apparent pulse period before being written to disk. Dedispersion (of 32 channels across the 128 MHz bandwidth) was carried out during data reduction, and appropriate phase bins were then chosen to generate on- and off-pulse images.

Data were edited and calibrated using the MIRIAD and AIPS packages according to standard procedures (Greisen 1996; Sault & Killeen 1998). On- and off-pulse images of a field containing each pulsar were formed using uniform weighting. Each image was deconvolved using either the CLEAN algorithm (for fields containing primarily point sources) or a maximum entropy algorithm (for fields containing significant extended emission), and then smoothed with a Gaussian restoring beam. For some sources the region was significantly confused by extended structure; in these cases, we constrained the deconvolution process by generating CLEAN boxes from lower resolution Molonglo Galactic Plane Survey (MGPS) or Northern VLA Sky Survey (NVSS) data (Green et al. 1999; Condon et al. 1998).

For each source, the position of the pulsar was determined by fitting in the $u-v$ plane to the difference of the on- and off-pulse data. For VLA data, a flux density for each

pulsar was determined by measuring a flux in the on-pulse image, then scaling using the width of the gate used. For ATCA data, flux densities were measured directly from ungated data. The sensitivity of each image was determined by measuring the off-pulse RMS at the pulsar position in each case.

3 RESULTS

The positions, fluxes and off-pulse sensitivities for the 27 pulsars observed are listed in Table 1, along with the range of spatial scales to which each image was sensitive. In most cases, the pulsar was clearly detected in the on-pulse image, and was completely gated out in the off-pulse image.

As a test of our sensitivity we included PSR B1706–44 in our VLA observations, a pulsar which is known to be embedded in a candidate PWN (Frail, Goss & Whiteoak 1994). This nebula was easily detected in our image, with a surface brightness and spatial extent similar to that obtained in previous data.

All but three of the pulsars in our sample were detected in these observations. For detections the measured interferometric position was compared with the timing position given in the pulsar catalogue (Taylor, Manchester & Lyne 1993). Our gated position for PSR B1706–44 differs significantly from the original timing position (Johnston et al. 1992), but is in reasonable agreement with the interferometric measurements of Frail, Goss & Whiteoak (1994) and the new timing position of Wang et al. (2000). Our position for

PSR B1754–24 has significantly smaller uncertainties than the catalogued position. The error in the latter is certainly much greater than the beamwidth in the observations of Kijak et al. (1998), and can account for their 4.9 GHz non-detection of this flat-spectrum pulsar. The majority of the remaining positions are consistent, to within 3σ , with positions determined from pulsar timing.

For the majority of sources in our sample, the off-pulse image showed no emission, extended or point-like, at or near the position of the pulsar. Sources of note are discussed individually below:

B0114+58: On-pulse data were corrupted for this source by hardware problems during the observations, and so no detection of the pulsar was made. The off-pulse image was uncorrupted, and shows no emission at the catalogued pulsar position.

B0136+57: An unresolved source of flux density 2.6 ± 0.3 mJy, approximately half of the observed pulsar flux density, is seen at the pulsar’s position in an off-pulse image. This source is $\sim 90\%$ linearly polarized, which is similar to the degree of polarisation seen for the pulsar (Gould & Lyne 1998). Thus the source probably corresponds to a component of the pulse-profile which was not properly gated out when the gate was set during observations.

J0631+1036: Images of the region were badly corrupted by sidelobes from the source 4C+10.20 (flux density 2.5 Jy), 19’ distant. The pulsar was not detected, its tabulated 1.4 GHz flux density of 0.8 mJy being below the sensitivity of the data. No other emission at or near the pulsar’s position was detected, down to the sensitivity limit.

B0656+14: No off-pulse emission is apparent at the pulsar’s position, but an extended, polarized source is seen $\sim 2'$ south of the pulsar, which Cordova et al. (1989) argue is possibly associated with the pulsar. We note that we see no connecting structure between the pulsar and this source, despite being more sensitive to extended emission than Cordova et al. (1989). It thus seems likely that this source is unrelated to the pulsar. We note that an X-ray PWN associated with this source was claimed by Kawai & Tamura (1996), but has been discredited by higher resolution data (Becker et al. 1999).

B1356–60: The region around this pulsar is shown in Fig 1 – the pulsar lies on the western rim of a shell of radio emission. This shell, which we designate G311.28+1.09, is approximately circular, with a diameter ~ 9 arcmin and a flux density 0.04 ± 0.01 Jy at 1.4 GHz. In linear polarization there is significant confusion from other sources in the region, and so it is not possible to determine whether the shell is polarized. Based on morphology alone, we thus consider G311.28+1.09 to be a possible new SNR, although further observations will be required to confirm this. However, given the 300-kyr characteristic age of the pulsar, it is unlikely that there is any physical association between PSR B1356–60 and G311.28+1.09. In an ungated image, no PWN is apparent around the pulsar, although the sensitivity to such a source is poor due to the presence of G311.28+1.09.

B1508–57: This pulsar is in a confused region of the Galactic Plane. We were forced to discard short $u-v$ spacings in order to image the region, limiting the largest spatial scale to which these observations were sensitive to only 1'.8. No off-pulse emission was observed, subject to this constraint.

B1634–45: The pulse profile for this source reveals an inter-

pulse separated in phase by 180 degrees from the main pulse, a result which has been confirmed by recent timing observations (F. Crawford, private communication). Gating out both the pulse and interpulse reveals an unresolved off-pulse source at the pulsar’s position of flux density 0.8 ± 0.4 mJy. This source is $\sim 80\%$ linearly polarized, similar to that measured for the main pulsed component. Since no PWN has ever been observed to be so highly polarized, we think it unlikely that this off-pulse source corresponds to an extended nebula; it is more likely that this emission comes from the pulsar itself. While we cannot rule out an error in the gating hardware or software, we note that no other gated ATCA observations have shown such an effect (see SGJ99). Alternatives are that there is a low-level bridge of pulsed emission connecting the two main components of the pulse profile (cf. PSR B1259–63; Manchester & Johnston 1995), or that the pulse profile contains an underlying unpulsed component (cf. PSR J0218+4232; Navarro et al. 1995). We are planning further ATCA observations of this source in order to distinguish between these possibilities.

B1706–16: An unresolved off-pulse source of flux density 4.0 ± 0.3 mJy is seen at the pulsar’s position. This source is less than 15% linearly or circularly polarized, but so is the pulsar itself (Gould & Lyne 1998). While the pulse profile is quite narrow and shows no evidence for an interpulse, the fact that the VLA gating is set on-line means that, as for PSR B0136+57, we are unable to rule out a component of the pulse profile as the source of this detection. As for PSR B1634–45 above, we plan to re-observe this pulsar with the ATCA in order to clarify this situation.

B1718–35: This pulsar is in a complicated region, and suffers significant confusion from the nearby star-forming region NGC 6334 (e.g. Brooks & Whiteoak 2000). Gating shows the pulsar to be located at the center of a 4’ radio nebula, G351.70+0.66, which is also clearly visible in data from the MGPS (Green et al. 1999). This region has a distinct counterpart at 60 μm in *IRAS* data, and is probably thermal.

B1727–33: Two ultra-compact H II regions are in the field, one of which, G354.19–0.06 (Becker et al. 1994), has a flux density of 0.3 Jy and is located $\sim 10'$ from the pulsar position. The pulsar was not detected, its catalogued flux of 2.9 mJy corresponding to a signal-to-noise of only 2σ .

B1730–37: The sensitivity of the observations was reduced by the presence of PMN J1733–3722 (flux density 0.6 Jy), just 2’ away.

B1754–24: The 1σ uncertainty in the right ascension of this pulsar was previously 14’; as discussed above, we have now greatly improved on this position. This more precise position puts the pulsar along the same line of sight as the large diffuse H II region G5.33+0.08 (Lockman, Pisano & Howard 1996). Emission from the latter is clearly seen in NVSS data and in the 90 cm image of Frail, Kassim & Weiler (1994), but is largely resolved out by our observations.

4 DISCUSSION

As discussed in §1, the parameters of the current survey were chosen to improve on the sensitivity of previous surveys, in particular that carried out by FS97. These factors are summarised in Fig 2, where the sensitivity of FS97’s search is compared to that presented here. Only for PWN with radii

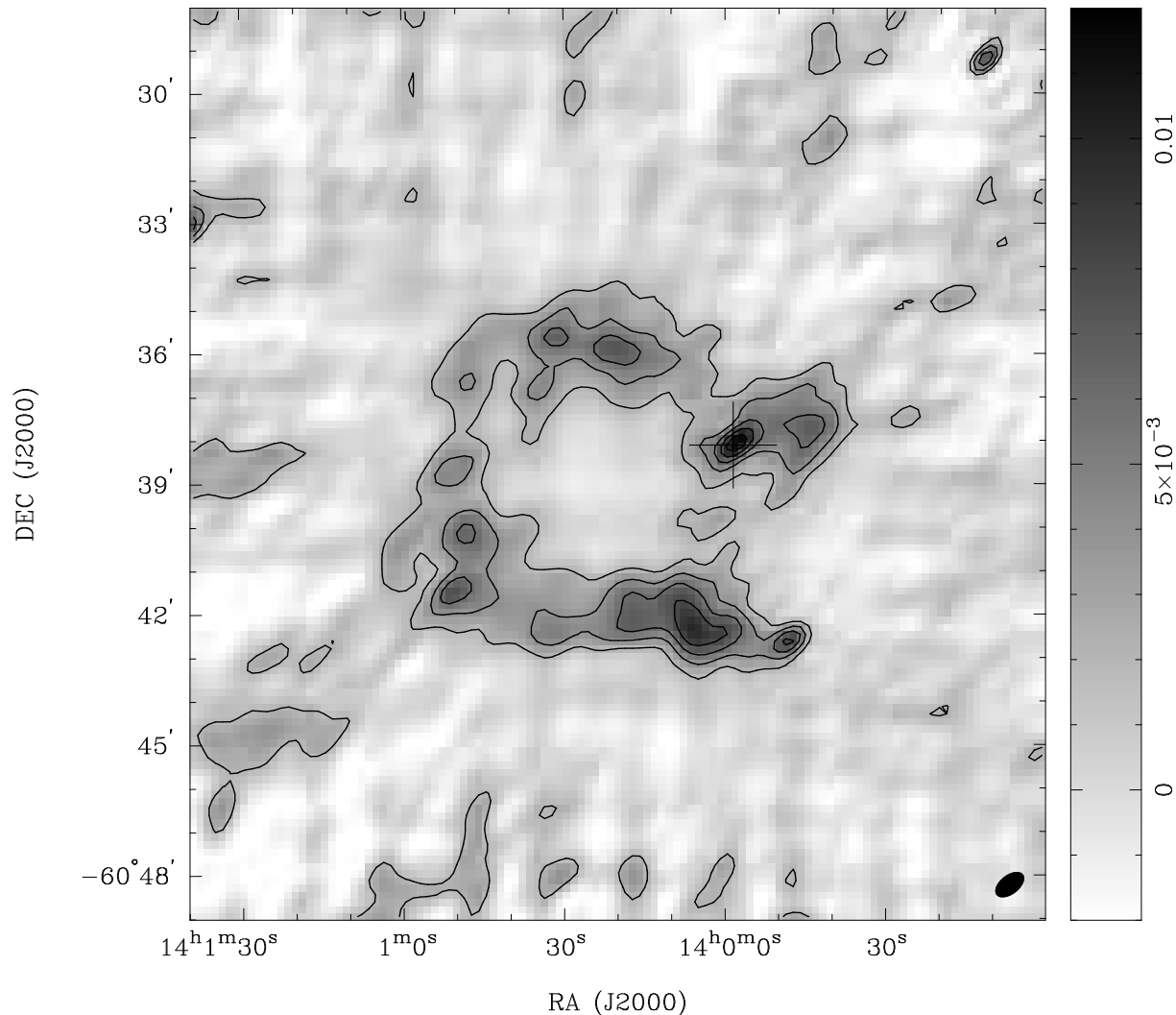


Figure 1. 1.4 GHz ATCA image of the region surrounding PSR B1356–60. Contours are at levels of 2, 4, 6, 8, 10 and 12 mJy beam^{−1}, at a resolution of 46'' × 26'' (FWHM shown at lower right). The pulsar (which has not been gated out in this image) is marked with a cross, and can be seen sitting on the western rim of the shell G311.28+1.09.

between 0'.4 and ∼ 1'' is FS97's search more sensitive than ours. Between 1'' and 10'', the current results are considerably (up to 100 times) more sensitive, while at scales smaller than 0'.4 and larger than 10'', our data probe a parameter space to which FS97 were not sensitive at all.

The results reported in §3 showed that most of the sources in our sample had no detectable PWN associated with them. The exceptions were PSRs B0136+57, B1634–45 and B1706–16, for which unresolved off-pulse sources were detected at the pulsar position. From the current data, we are unable to conclusively determine whether this emission corresponds to emission from the pulsar or from a compact PWN. While we plan to investigate these sources further, for the purposes of the present discussion we assume these observations to be non-detections, but with a sensitivity corresponding to the flux density of the off-pulse source (rather than to the noise in the surrounding area of the image).

To quantify the significance of our non-detections, we follow FS97 in characterising a radio PWN's integrated luminosity, L_R , by

$$L_R = \epsilon \dot{E} \text{ erg s}^{-1}, \quad (1)$$

where \dot{E} erg s^{−1} is the associated pulsar's spin-down luminosity, and ϵ is the fraction of \dot{E} which goes into radio emission.

Assuming a typical PWN spectral index $\alpha = -0.3$ and integrating from 10 MHz to 100 GHz, the corresponding 1.4 GHz flux density is

$$S_{1.4} = 2.1 \times 10^5 \frac{\epsilon \dot{E}_{34}}{d^2} \text{ mJy}, \quad (2)$$

where d kpc is the distance to the pulsar and $\dot{E} = 10^{34} \dot{E}_{34}$ erg s^{−1}. We generally use distances from the pulsar catalogue (Taylor et al. 1995), derived either from a pulsar's dispersion measure (Taylor & Cordes 1993) or from its kinematic distance based on H I measurements (e.g. Frail & Weisberg 1990).

If we do not detect a PWN in our observations, we can potentially put an upper limit on $S_{1.4}$, and hence on L_R and ϵ . However, as demonstrated in Fig 2, these limits depend on the angular size we expect for the PWN. As previously dis-

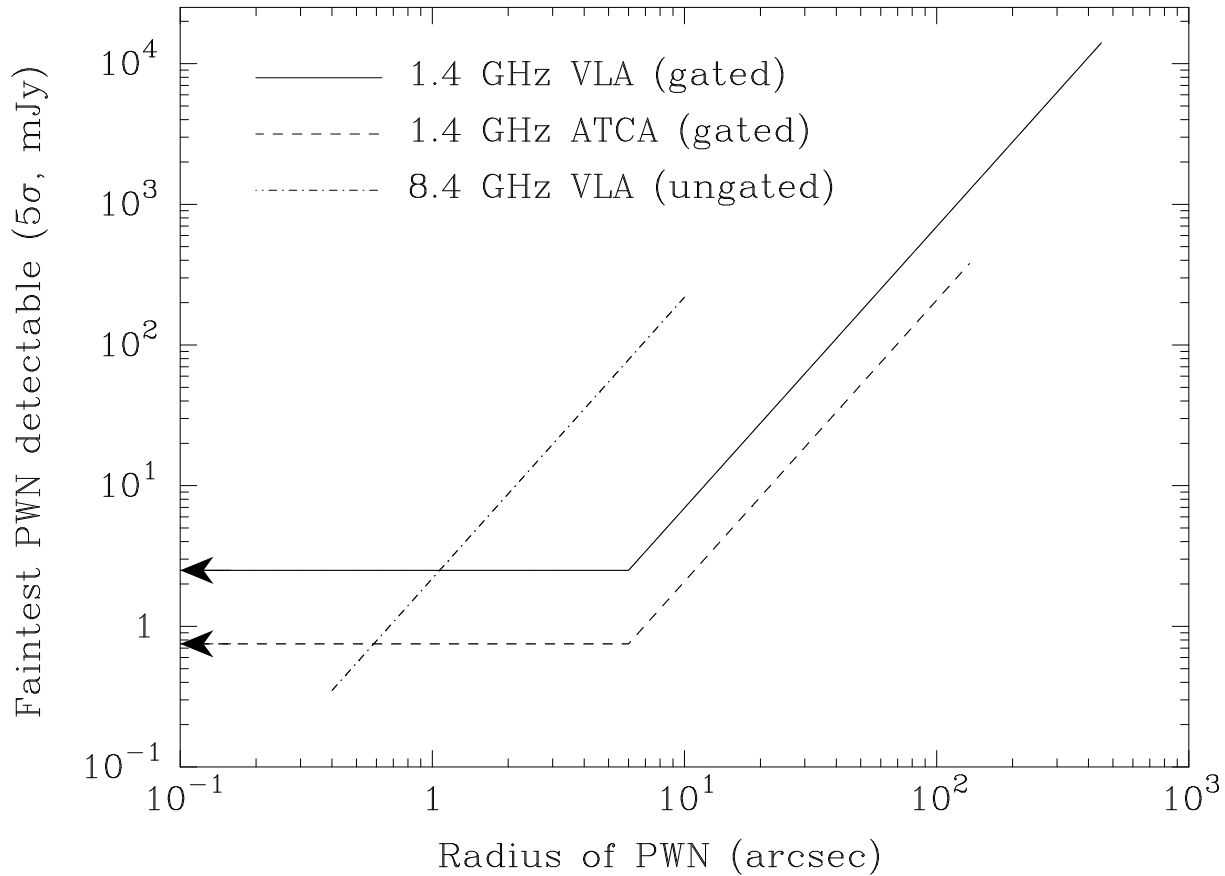


Figure 2. Comparison of 5σ sensitivities of the 8.4 GHz PWN search of FS97 with the 1.4 GHz observations reported here. The observations of FS97 were not gated, and so generally are not sensitive to PWN on scales smaller than the resolution limit. For our VLA (ATCA) observations, we have adopted a typical spatial resolution of $12''$ ($12''$), a maximum spatial scale of $15'$ ($4'5$), and a 1σ sensitivity of 0.5 (0.15) mJy beam^{-1} . A spectral index $\alpha = -0.3$ ($S_\nu \propto \nu^\alpha$) has been assumed in converting 8.4 GHz results to 1.4 GHz.

cussed by FS97 and SGJ99, PWN can in general be divided into two distinct classes (assuming that the pulsar is not inside a SNR, which appears to be the case for all the sources in our sample): those which are confined by the gas pressure of the ambient ISM (“static PWN”), and those confined by ram-pressure resulting from motion of the pulsar through the ISM (“bow-shock PWN”).

Let us first consider the case of a static PWN. The bubble in the ISM driven by the pulsar wind will expand supersonically into the ambient medium, producing a PWN of radius (Arons 1983)

$$R_{\text{static}} = 0.14 \times \left(\frac{\dot{E}_{34} t_3^3}{n} \right)^{1/5} \text{ pc}, \quad (3)$$

where $n \text{ cm}^{-3}$ is the density of the ambient medium (assumed to be pure hydrogen), and $t_3 \text{ kyr}$ is the period for which the pulsar has been interacting with the ISM. In further discussion we assume that this age is given by the pulsar’s characteristic age, $\tau_c \equiv P/2\dot{P}$.

However a PWN is only static while $\dot{R}_{\text{static}} > V_{\text{PSR}}$, where $V_{\text{PSR}} \text{ km s}^{-1}$ is the pulsar’s space velocity. Rearranging Equation (3) of FS97 (and correcting for a missing factor of 4π in their results), we find that a PWN will be static for velocities and ambient densities for which:

$$n V_{\text{PSR}}^5 \lesssim 4 \times 10^9 \dot{E}_{34} / t_3^2. \quad (4)$$

When this condition is not met, the pulsar has “overtaken” its own static PWN, and a bow-shock PWN results. The resulting PWN is much smaller than the static PWN, and has a size determined by a balance between the pressure of the relativistic pulsar wind and the ram-pressure resulting from the pulsar’s motion,

$$R_{\text{bow-shock}} = 0.63 \left(\frac{\dot{E}_{34}}{n V_{\text{PSR}}^2} \right)^{1/2} \text{ pc}, \quad (5)$$

where we have assumed that all the spin-down luminosity of the pulsar goes into the wind, and that the radius of a bow-shock PWN is 1.5 times the radius at which the ram and wind pressures balance (van Buren & McCray 1988).

Thus for a given n and V_{PSR} , we can use Equation (4) to determine whether a PWN has a static or a bow-shock morphology, and from this use either Equation (3) or (5) to determine its radius, and hence its angular extent, θ_{PWN} .

For a pulsar-gated observation with a 1.4 GHz RMS sensitivity of $\sigma \text{ mJy beam}^{-1}$ at a resolution $\theta'_\alpha \times \theta'_\delta$, suppose no off-pulse source is detected at the 5σ level. There are three possible reasons for this non-detection: the PWN is unresolved and below the point-source sensitivity of the observations, the PWN is resolved and below the surface

brightness sensitivity limit, or the PWN is larger than the maximum spatial scale to which we are sensitive. We now consider what limits on ϵ can be derived for each situation.

If θ_{PWN} is smaller than the resolution limit, then $S_{1.4} < 5\sigma$ and from Equation (2) the corresponding upper limit on ϵ is

$$\epsilon < \epsilon_0 = 2.4 \times 10^{-5} \sigma \left(\dot{E}_{34}/d^2 \right)^{-1}. \quad (6)$$

Note that if an off-pulse point source of 1.4 GHz flux density S_{pt} is detected at the position of the pulsar (as was the case for three of the pulsars in our sample), then 5σ should be replaced by S_{pt} in this expression.

If the PWN is extended, but smaller than the largest spatial scale to which our interferometer is sensitive, then

$$\epsilon < \frac{\epsilon_0 \theta_{\text{PWN}}^2}{\theta_\alpha \theta_\delta}, \quad (7)$$

where we have assumed a Gaussian profile for the PWN. Finally, if the PWN is larger than our observations can detect, we can put no limit on ϵ .

FS97 have argued, on the basis of their non-detections, that the lack of observable radio PWN around most pulsars implies $\epsilon \lesssim 10^{-6}$, two orders of magnitude less than for pulsars with detected radio PWN. However, in making this calculation they assumed that the ambient density was $n = 1 \text{ cm}^{-3}$. Through Equation (4), when combined with a reasonable velocity, this implied that all the pulsars they observed were powering bow-shock PWN, and the consequent high ram pressure ensured that these sources would largely be unresolved by their $0''.8$ resolution.

However their assumed ambient density is not representative of our current best understanding of the ISM. While the relative filling fractions are uncertain, available evidence supports a multi-phase ISM of which 90% by volume is a combination of a warm medium of density $n = 0.3 \text{ cm}^{-3}$ and a hot ionised component of density $n = 0.003 \text{ cm}^{-3}$ (see Ferrière 1998a for a recent discussion and overview). In the hot low-density component, we still expect most PWN to be bow shocks, but the ram pressure is greatly reduced and PWN will consequently be much more extended. Thus many PWN in this low density medium will be larger than the resolution limit of FS97, and through Equation (7), the limit on ϵ much less stringent than claimed.

In order to better consider the limits on ϵ , we therefore carry out the following calculation for 27 of the pulsars in Table 1 (PSR B1706–44 is excluded as it has a candidate PWN), and additionally for the 4 pulsars discussed by SGJ99. For each pulsar in our sample, we adopt possible densities of $n = 0.3 \text{ cm}^{-3}$ and $n = 0.003 \text{ cm}^{-3}$. Ten of the pulsars in our sample have measured proper motions, and we use the corresponding 3D space velocities determined by Cordes & Chernoff (1998); one other pulsar (PSR B1055–52) has had a scintillation velocity determined for it (Johnston, Nicastro & Koribalski 1998). For the remaining sources we set $V_{\text{PSR}} = 380 \text{ km s}^{-1}$, corresponding to the mean pulsar velocity of the distribution of Cordes & Chernoff (1998). Using Equation (4) we determine whether each corresponding PWN is bow-shock or static, and then consequently determine θ_{PWN} . Upper limits on ϵ are then determined from Equations (6) and (7), and the results given in Table 2. For the 16 sources in our sample which were also observed by FS97, we can make a similar calculation based on their re-

sults (converting their data to 1.4 GHz assuming a spectral index $\alpha = -0.3$); these revised values of ϵ_{max} are also listed in Table 2. Note that many PWN are unresolved for either choice of ambient density, and so have the same value of ϵ_{max} in both cases.

We can compare our upper limits to values of ϵ for known PWN. In Table 3 of FS97, ϵ is listed for the six pulsars then known to have detected radio PWN, to which we add PWN which have since been associated with PSR J0537–6910 ($\epsilon = 5 \times 10^{-4}$; Lazendic & Dickel 1998), PSR B0906–49 ($\epsilon = 2 \times 10^{-6}$; GSFJ98) and PSR J1811–1926 ($\epsilon < 2 \times 10^{-3}$; Morsi & Reich 1987; Torii et al. 1999). For these nine sources, six measurements lie in the reasonably narrow range $(1 - 5) \times 10^{-4}$. Those sources lying outside this range are PSR B0833–45, for which it is unclear just what part of the surrounding SNR is pulsar-powered, PSR B0906–49, which GSFJ98 argue is substantially different from other PWN, and PSR J1811–1926, where the radio PWN is faint and has poorly constrained properties. Thus the data available suggest that a “typical” detectable PWN has $\epsilon \approx 10^{-4}$.

FS97 argued that typical non-detections corresponded to $\epsilon_{\text{max}} \sim 2 \times 10^{-6}$, significantly less than for detected PWN. However, it can be seen from the results in Table 2 that for $n = 0.003 \text{ cm}^{-3}$ some PWN become too large to be detected by their data, while for the remaining pulsars the limit rises to $\epsilon_{\text{max}} \sim 3 \times 10^{-4}$. Thus we argue that the observations of FS97 could have missed “normal” PWN around most of their sample if most of these sources are in low density regions, and hence their observations do not constrain pulsars which lack detectable PWN to be any different in their wind properties from those pulsars with observed PWN.

On the other hand, the current observations can potentially provide constraining limits on ϵ . We first consider the six young and energetic pulsars in our sample (i.e. the first six pulsars in Table 2). These pulsars are defined approximately by $\dot{E}_{34} \gtrsim 50$ and $t_3 \lesssim 50$, properties similar to those pulsars with detectable radio PWN. For either assumed ISM density, our data constrain these pulsars to have upper limits on ϵ in the range $(0.002 - 0.2) \times 10^{-4}$, significantly less than for pulsars with observed PWN. While this seems to imply genuinely low values of ϵ , for $n = 0.003 \text{ cm}^{-3}$, conditions are such that these pulsars have only recently overtaken their static nebulae. Lowering their velocities slightly, arguing that their actual ages are less than their characteristic ages, or accepting that realistically, the transition from static to bow-shock PWN does not happen instantaneously, it seems likely that these pulsars are still producing static nebulae, whose extents are much larger than for bow-shocks. In this case, the corresponding limits become $\epsilon_{\text{max}} \gg 10^{-4}$, and are not constraining.

We thus argue that our non-detections of PWN can be explained even if all young and energetic pulsars have similar wind properties. The difference between detectable and non-detectable PWN seems to be that detected PWN are either in dense regions of the ISM or in SNRs, in which there is sufficient external pressure to confine the pulsar wind and produce an observable PWN. However, pulsars with no PWN are in the low density phase of the ISM and so produce unobservable “ghost remnants” (Blandford et al. 1973). With the exception of PSR B0906–49 (GSFJ98), pulsars with observed PWN also have associated SNRs, while all those young pulsars without PWN also have no associ-

Table 2. Upper limits on $\epsilon = L_R/\dot{E}$ for PWN non-detections, including four non-detections from SGJ99. Pulsars are sorted by decreasing \dot{E} ; θ is the predicted angular size of a PWN for a given density. For upper limits on ϵ derived from the results of FS97, U indicates that the predicted size of the PWN is too large to have been detected by their observations, while “...” indicates that a particular pulsar was not part of their sample.

Pulsar	\dot{E}_{34} (erg s ⁻¹)	t_3 (kyr)	d (kpc)	V_{PSR} (km s ⁻¹)	θ (")	$n = 0.3 \text{ cm}^{-3}$		$n = 0.003 \text{ cm}^{-3}$		
						$\log_{10} \epsilon_{\text{max}}$ (this paper)	$\log_{10} \epsilon_{\text{max}}$ (FS97)	θ (")	$\log_{10} \epsilon_{\text{max}}$ (this paper)	$\log_{10} \epsilon_{\text{max}}$ (FS97)
B1823-13	280	21	4.1	...	5.01	-6.3	-5.4	50.1	-5.2	U
J1105-6107	250	63	7.1	...	2.76	-5.8	...	27.6	-5.6	...
B1046-58	200	20	3.0	...	5.86	-6.8	...	58.6	-5.3	...
B1610-50	160	7	7.2	...	2.16	-5.8	...	21.6	-5.3	...
B1727-33	120	26	4.2	...	3.19	-5.2	-5.3	31.9	-4.8	U
B1930+22	75	40	12.1	...	0.88	-4.6	-5.4	8.8	-4.6	-3.4
B0114+58	22	275	2.1	...	2.70	-5.6	-5.4	27.0	-5.1	U
J1835-1106	18	127	3.1	...	1.69	-5.1	...	16.9	-5.0	...
J0631+1036	17	44	6.6	...	0.78	-4.0	...	7.8	-4.0	...
B0740-28	14	157	1.9	276	3.36	-5.5	-4.6	33.6	-4.9	U
B1508-57	13	298	12.7	...	0.35	-4.2	...	3.5	-4.2	...
B1356-60	12	319	5.9	...	0.72	-4.7	...	7.2	-4.7	...
B1634-45	7.5	590	3.8	...	0.88	-5.1	-5.3	8.8	-5.1	-3.3
B0611+22	6.3	89	4.7	212	1.18	-4.5	-4.9	11.8	-4.5	-2.9
J0538+2817	4.9	619	1.8	...	1.54	-5.2	...	15.4	-5.0	...
B1718-35	4.5	176	6.4	...	0.41	-3.5	...	4.1	-3.5	...
B0355+54	4.5	563	2.1	210	2.29	-5.2	-4.8	22.9	-4.7	U
B0540+23	4.1	253	3.5	348	0.77	-4.5	-5.1	7.7	-4.5	-3.3
B1754-24	4.0	285	3.5	...	0.71	-5.0	...	7.1	-5.0	...
B0656+14	3.8	111	0.8	331	3.63	-6.0	-5.2	36.3	-5.1	U
B1719-37	3.3	345	2.5	...	0.89	-4.6	-5.4	8.9	-4.6	-3.4
B1821-19	3.0	574	5.2	...	0.41	-4.4	-4.7	4.1	-4.4	-3.3
B1055-52	3.0	535	1.5	440	1.21	-5.8	...	12.1	-5.7	...
B2011+38	2.9	412	13.1	...	0.16	-2.9	-4.0	1.6	-2.9	-3.4
B0136+57	2.1	403	2.9	340	0.69	-4.3	-4.6	6.9	-4.3	-3.3
B1449-64	1.9	1035	1.8	337	1.04	-5.5	...	10.4	-5.5	...
B1730-37	1.5	355	3.5	...	0.44	-3.6	...	4.4	-3.6	...
B1933+16	0.51	947	7.9	996	0.04	-3.0	...	0.4	-3.0	...
B1706-16	0.12	1655	1.3	186	0.59	-3.5	...	5.9	-3.5	...
B0736-40	0.089	3805	2.1	377	0.21	-3.8	...	2.1	-3.8	...
B2148+63	0.012	36640	13.6	...	0.01	-0.7	-1.6	0.1	-0.7	-1.6

ated SNRs. We indeed expect SNRs to be undetectable in the hot component of the ISM (Kafatos et al. 1980; Gaensler & Johnston 1995), consistent with our conclusion above that it is a low ambient density which causes a PWN around a young pulsar to be undetectable.

A notable exception is PSR B1757-24, which is associated with both a SNR and a radio PWN despite having $n = 0.003 \text{ cm}^{-3}$ (Frail & Kulkarni 1991; Manchester et al. 1991). In this case, the pulsar is inferred to have a transverse space velocity $\sim 1500 \text{ km s}^{-1}$ (Frail, Kassim & Weiler 1994); this not only supplies the necessary ram pressure to produce an observable PWN, but has caused the pulsar to overtake the shell of the associated SNR, re-energising the remnant with its passage. If it were not for the extreme velocity of the pulsar, neither the PWN nor the SNR would be detectable, as expected in a low density region.

The relative numbers of young pulsars with detected and undetected SNRs/PWN suggests an approximate filling fraction $\sim 50\%$ for the low density component of the ISM. This is somewhat more than recent estimates of 15–20% (Ferrière 1998b), but can be explained by the fact that we expect young pulsars to be preferentially located in low density regions produced by the powerful winds of their progenitors and by previous supernovae in the region.

The majority of pulsars in our sample are considerably

less energetic ($\dot{E}_{34} < 50$) and older ($t_3 \gtrsim 100$) than pulsars around which radio PWN have been observed. Values of ϵ_{max} for these pulsars are plotted in Fig 3, from which it can be seen that for either choice of ambient density, the distribution peaks around $\epsilon_{\text{max}} \sim 10^{-5}$. These pulsars have all long since overtaken their static PWN, and will have bow shock PWN for any sensible choice of n and V_{PSR} . The resulting size of such a PWN is not a strong function of n or V_{PSR} ; to produce values of $\epsilon_{\text{max}} > 10^{-4}$, consistent with detected PWN, requires uniformly low space velocities, $V_{\text{PSR}} \lesssim 150 \text{ km s}^{-1}$, for these pulsars. However, only $\sim 5\%$ of pulsars are thought to be traveling at less than 150 km s^{-1} (Cordes & Chernoff 1998). While the ages and distances we have used for these pulsars have their associated uncertainties, for bow-shock PWN values of ϵ_{max} are independent of age, and distances would have to uniformly be increased by a factor of three to shift the peak in ϵ_{max} to a value in agreement with that seen for detected PWN. The lower value of ϵ we have derived for older pulsars is thus a result quite robust to the assumptions and uncertainties involved in its derivation, and we therefore argue that these pulsars have winds which are genuinely at least an order of magnitude less efficient at producing radio emission than the winds of young and energetic pulsars.

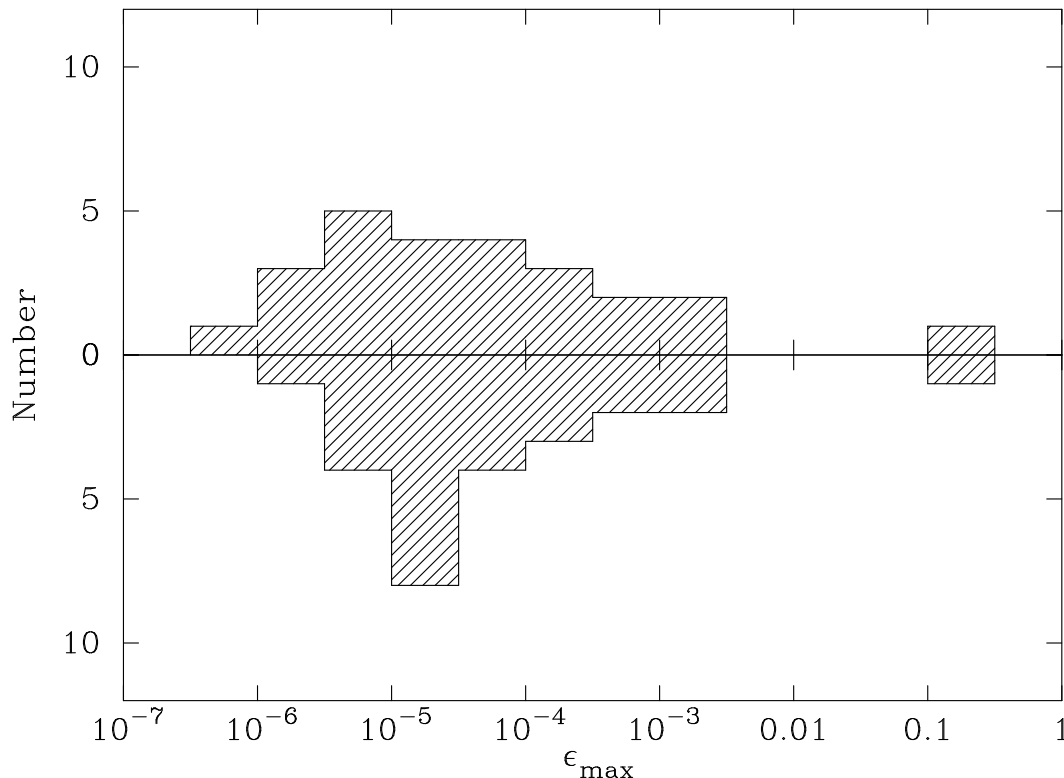


Figure 3. Upper limits on $\epsilon = L_R/\dot{E}$ from pulsar-gated 1.4 GHz data in Table 2; pulsars with $\dot{E}_{34} > 50$ have been excluded. The upper panel corresponds to an assumed ambient density $n = 0.3 \text{ cm}^{-3}$, while the lower panel represents $n = 0.003 \text{ cm}^{-3}$.

FS97 consider various reasons why older pulsars might appear to have lower values of ϵ . Possibilities include:

- (i) that the PWN are resolved out by the observations;
- (ii) that an increasing fraction of \dot{E} goes into pulsed X-rays and γ -rays (see Thompson et al. 1994);
- (iii) that their winds are dominated by Poynting flux rather than relativistic particles;
- (iv) that the injection spectrum of particles in the pulsar wind has shifted to higher energies.

Our observations can conclusively rule out alternative (i), as we can detect PWN produced for almost all feasible values of n and V_{PSR} . While we cannot distinguish between the remaining three possibilities, we note that of detected PWN, that associated with the oldest pulsar, PSR B0906–49, also has the lowest value of ϵ and the steepest spectral index (GSFJ98). Since the spectral index of a PWN is directly related to the spectrum of injected particles (Pacini & Salvati 1973), this result tentatively suggests that the efficiency of the wind in producing radio emission is related to the injection spectrum, and that alternative (iv) might then best explain the observations.

CONCLUSIONS

We have used pulsar-gating at 1.4 GHz to search for radio PWN around 27 pulsars. Our search was up to 100 times more sensitive than the only other comparable survey, and was carried out on spatial scales corresponding to a much

wider range of ambient densities and pulsar velocities. Including data from previous work by SGJ99, non-detections towards 28 pulsars, plus inconclusive results in three other cases, have allowed us to determine upper limits on ϵ , the fraction of a pulsar’s spin-down luminosity which goes into producing radio emission from a PWN.

We find that the data are consistent with virtually all young energetic pulsars having $\epsilon \sim 10^{-4}$. The lack of PWN around $\sim 50\%$ of young pulsars can be explained if they are in low ambient densities (0.003 cm^{-3}), consistent with the absence of associated supernova remnants around these sources.

For older pulsars, any reasonable choice of ambient density and pulsar velocity results in upper limits on the wind efficiency $\epsilon < 10^{-5}$, ten times less than for young pulsars. Thus pulsars seem to become less efficient at producing radio wind nebulae as they age; we speculate that this result is due to the spectrum of injected relativistic particles steepening in older pulsars. This possibility can be tested through X-ray observations towards such pulsars – it is likely that *Chandra* will make many new detections of X-ray PWN, and through consequent imaging spectroscopy, we may finally be able to probe the winds around older pulsars.

Of the ~ 55 non-recycled pulsars with $\dot{E} > 3 \times 10^{34} \text{ erg s}^{-1}$, almost all have now been searched for associated radio PWN down to a good sensitivity. If those sources with no detectable PWN are indeed in low density regions of the ISM, it seems unlikely that we will ever find radio PWN around them with current telescopes. For example, if PSR B1046–58 is powering a static PWN with $\epsilon = 10^{-4}$,

the resulting radio nebula would be 20' across with a flux density at 1.4 GHz of 0.5 Jy. To detect this source would require $\sigma = 0.3$ mJy arcmin⁻², which is generally below the confusion limit for instruments capable of imaging sources this large. We might have to wait for the large increase in sensitivity promised by the Square Kilometre Array in order to make further progress.

ACKNOWLEDGEMENTS

We are particularly grateful to Walter Brisken for his help with pulsar-gating at the VLA, Barry Clark and Miller Goss for their generous re-scheduling of a failed observing run, and Andrew Lyne for supplying timing solutions for many of the pulsars we observed. We also thank Phillip Hicks for his assistance with the observations, Froney Crawford for information on the pulse profile of PSR B1634–45, and Jon Arons, Jim Cordes, Vicky Kaspi, Michael Pivovarov and Eric van der Swaluw for useful discussions and suggestions. This research has made use of the data base of published pulse profiles maintained by the European Pulsar Network, available at <http://www.mpifr-bonn.mpg.de/pulsar/data>, NASA's Astrophysics Data System Abstract Service and of the SIMBAD database, operated at CDS, Strasbourg, France. The National Radio Astronomy Observatory is a facility of the National Science Foundation operated under cooperative agreement by Associated Universities, Inc. The Australia Telescope is funded by the Commonwealth of Australia for operation as a National Facility managed by CSIRO. B.M.G. acknowledges the support of NASA through Hubble Fellowship grant HF-01107.01-98A awarded by the Space Telescope Science Institute, which is operated by the Association of Universities for Research in Astronomy, Inc., for NASA under contract NAS 5–26555. B.W.S. is supported by NWO Spinoza grant 08-0 to E.P.J. van den Heuvel.

REFERENCES

- Arons J., 1983, *Nat*, 302, 301
 Becker R. H., White R. L., Helfand D. J., Zoonematkermani S., 1994, *ApJS*, 91, 347
 Becker W., Kawai N., Brinkmann W., Mignani R., 1999, *AA*, 352, 532
 Blandford R. D., Ostriker J. P., Pacini F., Rees M. J., 1973, *J&A*, 23, 145
 Brooks K. J., Whiteoak J. B., 2000, *MNRAS*, submitted
 Cohen N. L., Cotton W. D., Geldzahler B. J., Marcaide J. M., 1983, *ApJ*, 264, 273
 Condon J. J., Cotton W. D., Greisen E. W., Yin Q. F., Perley R. A., Taylor G. B., Broderick J. J., 1998, *AJ*, 115, 1693
 Cordes J. M., Chernoff D. F., 1998, *ApJ*, 505, 315
 Cordova F. A., Middleditch J., Hjellming R. M., Mason K. O., 1989, *ApJ*, 345, 451
 Ferrière K., 1998a, *ApJ*, 497, 759
 Ferrière K., 1998b, *ApJ*, 503, 700
 Frail D. A., Kulkarni S. R., 1991, *Nat*, 352, 785
 Frail D. A., Scharringhausen B. R., 1997, *ApJ*, 480, 364 (FS97)
 Frail D. A., Weisberg J. M., 1990, *AJ*, 100, 743
 Frail D. A., Goss W. M., Whiteoak J. B. Z., 1994, *ApJ*, 437, 781
 Frail D. A., Kassim N. E., Weiler K. W., 1994, *AJ*, 107, 1120
 Frater R. H., Brooks J. W., Whiteoak J. B., 1992, *J. Electr. Electron. Eng. Aust.*, 12, 103
 Gaensler B. M., Johnston S., 1995, *MNRAS*, 277, 1243
 Gaensler B. M., Stappers B. W., Frail D. A., Johnston S., 1998, *ApJ*, 499, L69 (GSFJ98)
 Gould D. M., Lyne A. G., 1998, *MNRAS*, 301, 235
 Green A. J., Cram L. E., Large M. I., Ye T., 1999, *ApJS*, 122, 207, (<http://www.astrop.physics.usyd.edu.au/MGPS/>)
 Greisen E., ed, 1996, *The AIPS Cookbook*. National Radio Astronomy Observatory, Charlottesville
 Johnston S., Nicastro L., Koribalski B., 1998, *MNRAS*, 297, 108
 Johnston S., Lyne A. G., Manchester R. N., Kniffen D. A., D'Amico N., Lim J., Ashworth M., 1992, *MNRAS*, 255, 401
 Kafatos M., Sofia S., Bruhweiler F., Gull S., 1980, *ApJ*, 242, 294
 Kawai N., Tamura K., 1996, in Johnston S., Walker M. A., Bailes M., eds, *Pulsars: Problems and Progress*, IAU Colloquium 160. Astronomical Society of the Pacific, San Francisco, p. 367
 Kennel C. F., Coroniti F. V., 1984, *ApJ*, 283, 710
 Kijak J., Kramer M., Wielebinski R., Jessner A., 1998, *AAS*, 127, 153
 Lazendic J. S., Dickel J. R., 1998, *Mem. S. A. It.*, 69, 843
 Lockman F. J., Pisano D. J., Howard G. J., 1996, *ApJ*, 472, 173
 Manchester R. N., Johnston S., 1995, *ApJ*, 441, L65
 Manchester R. N., Kaspi V. M., Johnston S., Lyne A. G., D'Amico N., 1991, *MNRAS*, 253, 7P
 Michel F. C., 1982, *Reviews of Modern Physics*, 54, 1
 Morsi H. W., Reich W., 1987, *A&AS*, 71, 189
 Napier P. J., Thompson A. R., Ekers R. D., 1983, *Proc. I. E. E. E.*, 71, 1295
 Navarro J., de Bruyn G., Frail D., Kulkarni S. R., Lyne A. G., 1995, *ApJ*, 455, L55
 Pacini F., Salvati M., 1973, *ApJ*, 186, 249
 Rees M. J., Gunn J. E., 1974, *MNRAS*, 167, 1
 Sault R. J., Killeen N. E. B., 1998, *The Miriad User's Guide*. Australia Telescope National Facility, Sydney, (<http://www.atnf.csiro.au/computing/software/miriad/>)
 Schönhardt R. E., 1974, *AA*, 35, 13
 Stappers B. W., Gaensler B. M., Johnston S., 1999, *MNRAS*, 308, 609 (SGJ99)
 Taylor J. H., Cordes J. M., 1993, *ApJ*, 411, 674
 Taylor J. H., Manchester R. N., Lyne A. G., 1993, *ApJS*, 88, 529
 Taylor J. H., Manchester R. N., Lyne A. G., Camilo F. 1995. Unpublished (available at <ftp://pulsar.princeton.edu/pub/catalog>)
 Thompson D. J. et al., 1994, *ApJ*, 436, 229
 Torii K., Tsunemi H., Dotani T., Mitsuda K., Kawai N., Kinugasa K., Saito Y., Shibata S., 1999, *ApJ*, 523, 69
 van Buren D., McCray R., 1988, *ApJ*, 329, L93
 Wang N., Manchester R. N., Pace R., Bailes M., Kaspi V. M., Stappers B. W., Lyne A. G., 2000, *MNRAS*, submitted.
 Weiler K. W., Panagia N., 1978, *AA*, 70, 419
 Weiler K. W., Goss W. M., Schwarz U. J., 1974, *AA*, 35, 473